Journal of Biomechanics 44 (2011) 607–613

Contents lists available at ScienceDirect

Journal of Biomechanics

journal homepage: www.elsevier.com/locate/jbiomech
www.JBiomech.com

Finding consistent strain distributions in the glenohumeral capsule between two subjects: Implications for development of physical examinations

Nicholas J. Drury [a], Benjamin J. Ellis [b], Jeffrey A. Weiss [b], Patrick J. McMahon [a], Richard E. Debski [a,*]

[a] Musculoskeletal Research Center, Department of Bioengineering, University of Pittsburgh, 405 Center for Bioengineering, 300 Technology Drive, Pittsburgh, PA 15219, USA
[b] Department of Bioengineering, University of Utah, Salt Lake City, UT, USA

ARTICLE INFO

Article history:
Accepted 10 November 2010

Keywords:
Shoulder
Glenohumeral joint
Finite element models
Ligament
Strain

ABSTRACT

The anterior-inferior glenohumeral capsule is the primary passive stabilizer to the glenohumeral joint during anterior dislocation. Physical examinations following dislocation are crucial for proper diagnosis of capsule pathology; however, they are not standardized for joint position which may lead to misdiagnoses and poor outcomes. To suggest joint positions for physical examinations where the stability provided by the capsule may be consistent among patients, the objective of this study was to evaluate the distribution of maximum principal strain on the anterior-inferior capsule using two validated subject-specific finite element models of the glenohumeral joint at clinically relevant joint positions. The joint positions with 25 N anterior load applied at 60° of glenohumeral abduction and 10°, 20°, 30° and 40° of external rotation resulted in distributions of strain that were similar between shoulders ($r^2 \geq 0.7$). Furthermore, those positions with 20–40° of external rotation resulted in capsule strains on the glenoid side of the anterior band of the inferior glenohumeral ligament that were significantly greater than in all other capsule regions. These findings suggest that anterior stability provided by the anterior-inferior capsule may be consistent among subjects at joint positions with 60° of glenohumeral abduction and a mid-range (20–40°) of external rotation, and that the glenoid side has the greatest contribution to stability at these joint positions. Therefore, it may be possible to establish standard joint positions for physical examinations that clinicians can use to effectively diagnose pathology in the anterior-inferior capsule following dislocation and lead to improved outcomes.

1. Introduction

The glenohumeral joint is the most dislocated major joint in the body, with the majority of dislocations occurring in the anterior direction at joint positions involving ~60° of glenohumeral abduction and external rotation (Cave et al., 1974; Hawkins and Mohtadi, 1991). The glenohumeral capsule, a continuous sheet of ligamentous tissue connecting the scapula and humerus, transfers loads in multiple directions during joint motion (Debski et al., 2003; Malicky et al., 2001; O'Brien et al., 1990). Stability provided by specific regions of the capsule is dependent on joint position (Burkart and Debski, 2002; Debski et al., 1999; Harryman et al., 1992; Moore et al., 2004; Musahl et al., 2006; O'Brien et al., 1990; Turkel et al., 1981), with each region of the capsule being loaded and unloaded throughout the range of motion. During abduction and external rotation, passive anterior stability is provided primarily by the anterior-inferior capsule (Brenneke et al., 2000; Burkart and Debski, 2002; Debski et al., 1999; Drury et al., 2007; Gerber and Ganz, 1984; Moore et al., 2010; Moore et al., 2008; Moseley and Overgaard, 1962; O'Brien et al., 1990; Ovesen and Nielsen, 1985; Turkel et al., 1981) but the specific amounts of external rotation at which stability is provided by different regions of the anterior-inferior capsule are unknown.

Following dislocation, clinicians use multiple methods for diagnosing capsule pathology such as patient history, diagnostic imaging, and arthroscopic examination; however, physical examinations are the most crucial step for diagnosing the location and extent of capsule pathology (Brenneke et al., 2000; Matsen et al., 1991; Pollock and Bigliani, 1993). In spite of their importance, physical examinations are unreliable since they are not standardized for joint position. This may result in misdiagnosis of capsule pathology, especially when differences in capsule function exist between patients (Tzannes et al., 2004). Misdiagnoses from physical examinations could then result in poor outcomes following surgery, since the location, extent, and type of repair are dependent on the location and extent of the capsule pathology (Gerber and Ganz, 1984; Moore et al., 2004; Rockwood et al., 1998). Over 38% of post-operative re-dislocations have been reported to be due to misdiagnoses of the location of capsule pathology, and 35% of post-operative re-dislocations and over 80% of post-operative pain, motion loss, and osteoarthritis cases have been shown to be due to misdiagnoses of the extent of capsule

* Corresponding author. Tel.: +1 412 648 2000; fax: +1 412 648 2001.
E-mail address: genesis1@pitt.edu (R.E. Debski).

0021-9290/$ - see front matter © 2010 Elsevier Ltd. All rights reserved.
doi:10.1016/j.jbiomech.2010.11.018

pathology (Cooper et al., 1992; Hawkins and Hawkins, 1985; Lusardi et al., 1993). Even though post-operative outcomes have improved over the last two decades (Boselli et al., 2010), misdiagnoses could still have a significant effect on the outcomes of surgery. These physical exams have been found to not be consistently reliable (May et al., 2010) and diagnosing subtle instability can be difficult (Cadet, 2010).

To improve physical examinations, joint positions need to be identified where the anterior stability provided by the capsule is consistent among subjects, i.e. where a high correlation exists among subjects in the manner of the distribution of load throughout the regions of the anterior-inferior capsule. Furthermore, these joint positions should also ensure that a single capsule region has a greater contribution to stability than the rest of the capsule, in that the load is primarily transferred by a single capsule region and the remaining regions are unloaded. Thus, clinicians could use these joint positions in physical examinations to effectively diagnose capsule pathology following dislocation.

Subject-specific finite element models of the glenohumeral joint provide a powerful tool for analyzing the multi-axial stability provided by the capsule among patients (Debski et al., 2005; Drury, 2008; Drury et al., 2007; Drury et al., 2008a; Ellis et al., 2006; Moore et al., 2010; Newman et al., 2002) using distribution of strain on the surface of the capsule as a measure of the distribution of load in the joint (Bigliani et al., 1992; Brenneke et al., 2000; Ellis et al., 2007; Kawada et al., 1999; Malicky et al., 2001; McMahon et al., 1999; Moore et al., 2005; Spalazzi et al., 2006). Therefore, the objective of this study was to evaluate the distribution of maximum principal strain on the anterior-inferior capsule in two validated subject-specific finite element models of the glenohumeral joint at clinically relevant joint positions. These data could be used to suggest preliminary joint positions for physical examinations where the stability provided by the capsule may be consistent among patients.

2. Materials and methods

2.1. Finite element model development and validation

Two subject-specific finite element models of the glenohumeral joint were developed, validated, and analyzed for the current study, to be referred to as Shoulder 1 and Shoulder 2. Using a combined experimental and computational approach, experimental data were obtained and used to develop and validate each model, using previously documented methodologies developed within our research center (Debski et al., 1999; Drury, 2008; Ellis et al., 2007; Ellis et al., 2010; Moore et al., 2010; Moore et al., 2008; Rainis et al., 2009). Therefore, only a brief description of the development and validation protocol is provided.

Each model was constructed using subject-specific inputs from a cadaver that included: (1) a reference position for use in determining capsule strains and joint kinematics, (2) geometry of the bones, capsule, and humeral head cartilage when the joint is at the reference position, (3) joint kinematics of the humerus with respect to the scapula from the reference position to clinically relevant joint positions with 25 N anterior load applied at 60° of glenohumeral abduction and 0°, 30°, and maximum external rotation, and (4) material coefficients of the capsule regions using an isotropic hyperelastic constitutive model to represent the capsule tissue. In addition, subject-specific distributions of strain on the anterior-inferior capsule were obtained at each joint position, for validation of the model. Shoulder 1 modeled a left shoulder from a 45 year old male, and Shoulder 2 modeled a right shoulder from a 66 year old male. Additional details of these experimental methods are provided in the online appendix and have been described previously (Debski et al., 1999; Drury, 2008; Ellis et al., 2007; Ellis et al., 2010; Moore et al., 2010; Moore et al., 2008; Rainis et al., 2009).

The three-dimensional surface geometry of the humerus, scapula, and humeral head cartilage were manually segmented on each slice of the CT dataset using SURFdriver (v3.5.6, Hawaii) and Amira (v 4.1.1, Mercury Computer Systems, Inc., Chelmsfor MA), as these structures provide the appropriate boundary conditions for the capsule during joint motion. Similarly, 3-dimensional surface geometries were obtained for the five capsule regions corresponding to the posterior region, anterosuperior region, and the three regions of the anterior-inferior capsule (AIC): the anterior band of the inferior glenohumeral ligament (AB-IGHL), the axillary pouch (AP), and the posterior band of the inferior glenohumeral ligament (PB-IGHL) (Moore et al., 2008; O'Brien et al., 1990). The surfaces were then imported into a finite element pre-processor (TrueGrid, XYZ Scientific, Livermore, CA). Surfaces representing the humerus, scapula, and humeral head cartilage were converted directly to rigid body meshes (Maker, 1995), and the bursal side of each capsule region was meshed with quadrilateral YASE shell elements due to their accuracy during bending deformations (Engelmann et al., 1989). Based upon experimental measurements of the AIC thickness, a 2.0 mm and 3.0 uniform thickness was prescribed to each capsule region for Shoulder 1 and Shoulder 2, respectively, and mesh densities were defined based on a previous study from our research group (Ellis et al., 2007). The glenoid labrum was simulated by increasing the thickness of the shell elements near the glenoid (Drury et al., 2008b), using experimental measurements of labrum thickness in the cadavers. The radial thicknesses of the elements representing the labrum were tapered linearly from 2.0 to 3.0 mm from the interfaces with the capsule and glenoid, respectively, for Shoulder 1, and from 3.0 to 6.0 mm for Shoulder 2.

Motions of the humerus with respect to the scapula were then prescribed using incremental translations and rotations based on the experimental kinematics (Simo, 1988). The nodes at the proximal and distal ends of the mesh of each capsule region were rigidly fixed to those of the humerus and scapula, and nodes between the capsule regions were joined in order to model the continuous nature of the capsule. A sliding interface with a tolerance value of 0.05 and a penalty value of 1.0 was prescribed between the nodes of the humeral head cartilage and the articular surface of the capsule to replicate the in-vivo contact between these surfaces.

The non-linear finite element solver FEBio (© Maas and Weiss, Salt Lake City, UT), was used for all analyses. The motions of the humerus with respect to the scapula were applied incrementally with the time step size being adjusted via an automatic procedure. Positions of the capsule strain markers used to create experimental elements for validation were incorporated into the model, so that predicted strains in the finite element models could be computed on areas of the capsule that corresponded to the size and location of the experimental validation elements. LSPOST (Livermore Software Technology Corporation, Livermore, CA) was then used to visualize and output predicted Green–Lagrange maximum principal strains on the computational validation elements, for direct comparison with the Green–Lagrange maximum principal strains obtained on the experimental validation elements.

Validation of each finite element model was performed by comparing predicted and experimental strains on the validation elements of the AIC at the three joint positions. The criterion for validation was that the average difference in strains between the experimental and computational models was less than the experimental repeatability of the testing system ($\pm$ 3.5% strain) (Moore et al., 2008).

2.2. Analysis of joint positions

Several joint positions that were examined using the finite element models were not obtained experimentally since capsule degradation limited the number of joint positions that could be examined with the robotic/UFS system. Therefore, the kinematics for these additional joint positions (25 N anterior load applied at 60° of abduction and 10°, 20°, 40°, and 50° of external rotation) were determined by linearly interpolating between the kinematics from the reference position to the three joint positions obtained experimentally (25 N anterior load applied at 60° of abduction and 0°, 30°, and maximum external rotation). For each set of kinematics associated with the experimentally obtained joint positions, the motion of the humeral registration block with respect to the scapular registration block was transformed into motion of the humerus with respect to the scapular anatomical coordinate systems defined on the robotic/UFS testing system. The kinematics of the additional joint positions were then obtained by linearly interpolating the joint motions (i.e. external rotation, anterior–posterior translation) between the

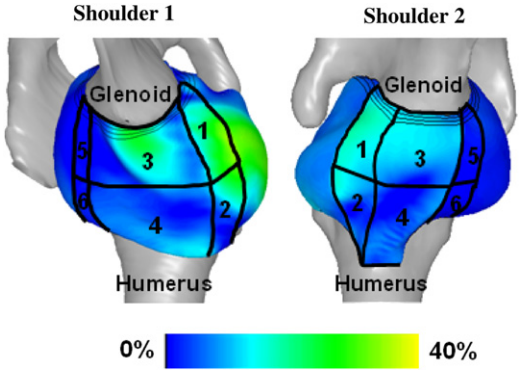

Fig. 1. Inferior views of Shoulder 1 (left shoulder) and Shoulder 2 (right shoulder) at the joint position with 25 N anterior load applied at 60° of glenohumeral abduction and 30° of external rotation, indicating the six sub-regions of the anterior-inferior capsule. 1 = AB-IGHL:G, 2 = AB-IGHL:H, 3 = AP:G, 4 = AP: H, 5 = PB-IGHL:G, 6 = PB-IGHL:H.

experimentally obtained joint positions. The kinematics for these additional joint positions were then transformed into the coordinate systems of the humeral and scapular registration blocks for subsequent input into the finite element models.

Predicted distributions of strain on the capsule were obtained by computing the Green–Lagrange maximum principal strain at the nodes of the shell elements representing the capsule at each joint position. Six sub-regions of the AIC were defined based upon previous work and clinical outcomes (Bankart, 1938; Bankart, 1923; Drury et al., 2007; Malicky et al., 2001; Moore et al., 2008, Bigliani et al., 1992; Itoi et al., 1993; Ticker et al., 1996) corresponding to the glenoid and humeral sides of the anterior band of the inferior glenohumeral ligament (AB-IGHL:G and

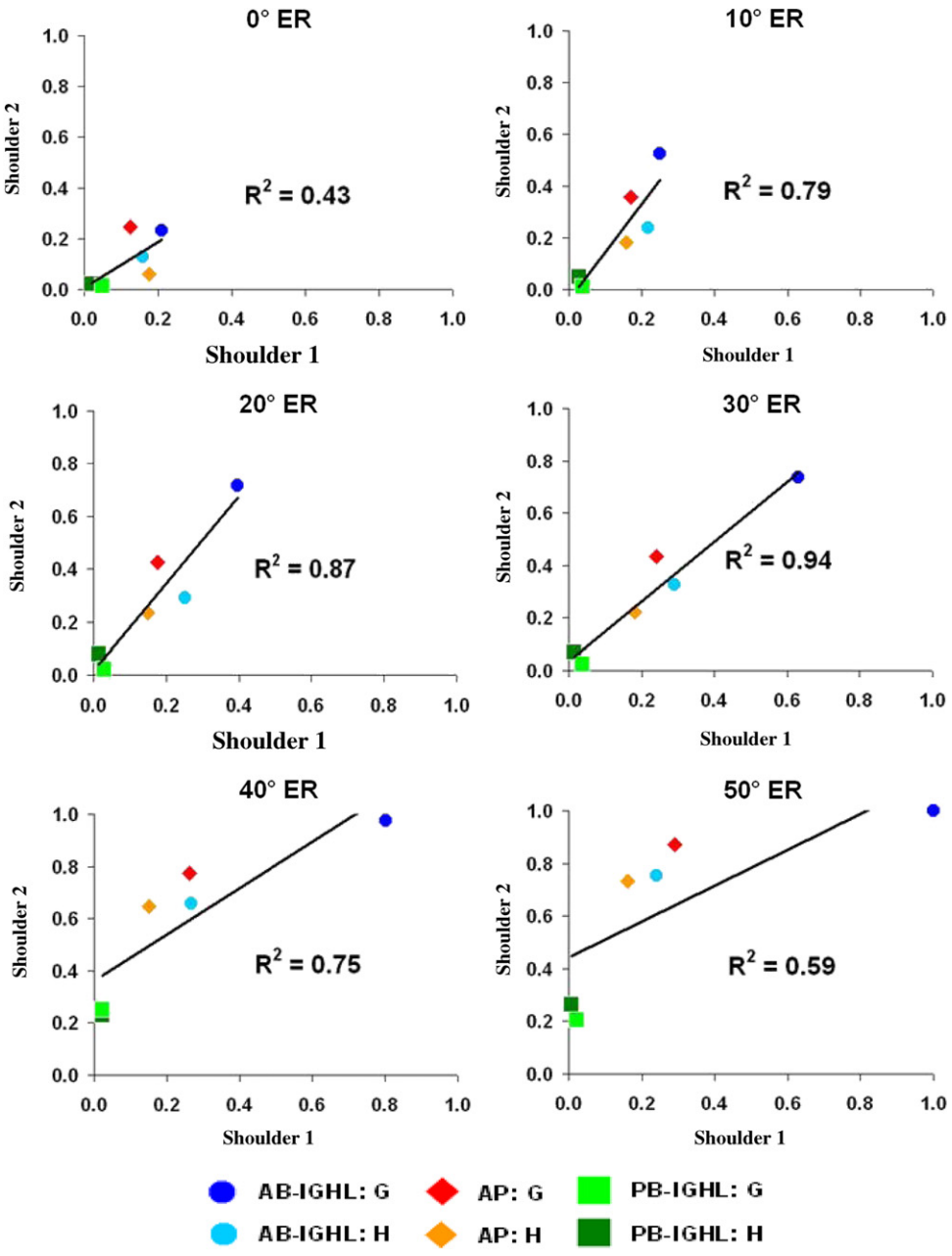

Fig. 2. Correlation of strain ratios in the sub-regions of the anterior-inferior capsule of Shoulder 2 vs. Shoulder 1, at each of the six joint positions. $r^2 \geq 0.7$ indicates high correlation between the distribution of strain on the anterior-inferior capsule in Shoulder 1 and Shoulder 2. G=glenoid, H=humerus.

Table 1
Experimental and predicted strains (Avg ± SD) in the validation elements of the anterior band of the inferior glenohumeral ligament, as well as the difference in experimental and predicted strains. Model validation requires that average differences are less than ±3.5% strain.

Joint position	Shoulder 1 Strains			Joint position	Shoulder 2 Strains		
	Exp. (%)	Pred. (%)	Diff. (%)		Exp. (%)	Pred. (%)	Diff. (%)
0° ER	18 ± 11	5 ± 3	−13	0° ER	8 ± 9	5 ± 1	−3
30° ER	19 ± 11	20 ± 10	1	30° ER	14 ± 15	15 ± 2	0
max (51.8°) ER	21 ± 14	23 ± 16	2	max (57.3°) ER	16 ± 15	17 ± 4	1

AB-IGHL:H, respectively), the axillary pouch (AP:G and AP:H, respectively), and the posterior band of the inferior glenohumeral ligament (PB-IGHL:G and PB-IGHL:H, respectively) (Fig. 1). The glenoid and humeral sub-regions were created by assigning elements to the glenoid or humeral side of the midway point between the glenoid and humeral insertions of the capsule. In both Shoulder 1 and Shoulder 2, predicted strains at the nodes were averaged within the six sub-regions at each joint position. This provided six values of strain at each joint position for both models.

The average nodal strains on the sub-regions in Shoulder 1 at a given joint position were then compared with those in Shoulder 2 at the equivalent joint position to determine joint positions with consistent distribution of strain on the AIC between the models. Since the magnitude of strain in the AIC is subject-specific but the manner in which strain is distributed throughout the AIC is similar among specimens (Moore et al., 2008), the highest average nodal strain on any sub-region at any of the joint positions was identified for each model, and the strains on the six sub-regions at each joint position were then normalized to this value. This process provided six ratios ranging from 0 to 1 at each joint position for both Shoulder 1 and Shoulder 2.

At each joint position the groups of six ratios in the two Shoulders were compared by determining a Pearson correlation coefficient using SPSS (Apache Software, 2000). A total of six correlation tests were performed based on the six shared joint positions of Shoulder 1 and Shoulder 2, corresponding to the joint positions with 0°, 10°, 20°, 30°, 40°, and 50° of external rotation. Squared correlation coefficients above 0.7 were reflective of high correlation (Munro, 2005). Therefore, joint positions with a $r^2 \geq 0.7$ were defined as having a consistent distribution of strain and thus consistent distribution of load between the two models. These joint positions were used for further analyses.

Since joint positions with relatively low transfer of load in the capsule are unhelpful for diagnoses, regardless of whether the distribution of load at these joint positions is consistent among subjects, the joint positions in which Shoulder 1 and Shoulder 2 did not have at least one sub-region with average strain greater than or equal to 7% strain (twice the experimental repeatability) were excluded from the analyses.

For the joint positions included in the analyses, the sub-region strains in the models were evaluated to determine if one sub-region of the AIC had significantly greater strain than the other sub-regions and thus the greatest contribution to stability. Specifically, in each model the values of strain on the six sub-regions were compared at each joint position using a Kruskal–Wallis test ($p < 0.05$) with Bonferroni-corrected Mann–Whitney tests for post-hoc analysis. Differences were determined to be significant (*) if they were statistically significant and on average greater than the experimental repeatability of $\pm 3.5\%$ strain. Joint positions were then identified that had a given sub-region with significantly greater strain than the other sub-regions in both Shoulder 1 and Shoulder 2.

3. Results

Validation of both Shoulder 1 and Shoulder 2 was completed using the validation elements in the AB-IGHL since this was the only region of the AIC that had experimental strains above the experimental repeatability of $\pm 3.5\%$ strain at the three joint positions. Due to subject-specific variability in the size of the AB-IGHL, eleven validation elements were used for Shoulder 1 and eighteen validation elements were used for Shoulder 2.

Shoulder 1 was validated at the joint positions with 30° and maximum (51.8°) external rotation, with differences in experimental and predicted strains on the validation determined to be 1% and 2% strain, respectively (Table 1). Shoulder 1 was unable to be validated at the joint position with 0° of external rotation as the difference was determined to be −13% strain. Shoulder 2 was validated at all of the joint positions (0°, 30°, and maximum (57.3°) external rotation), with differences in experimental and predicted strains on the validation elements determined to be −3%, 0%, and 1% strain, respectively. It is worth noting that while model

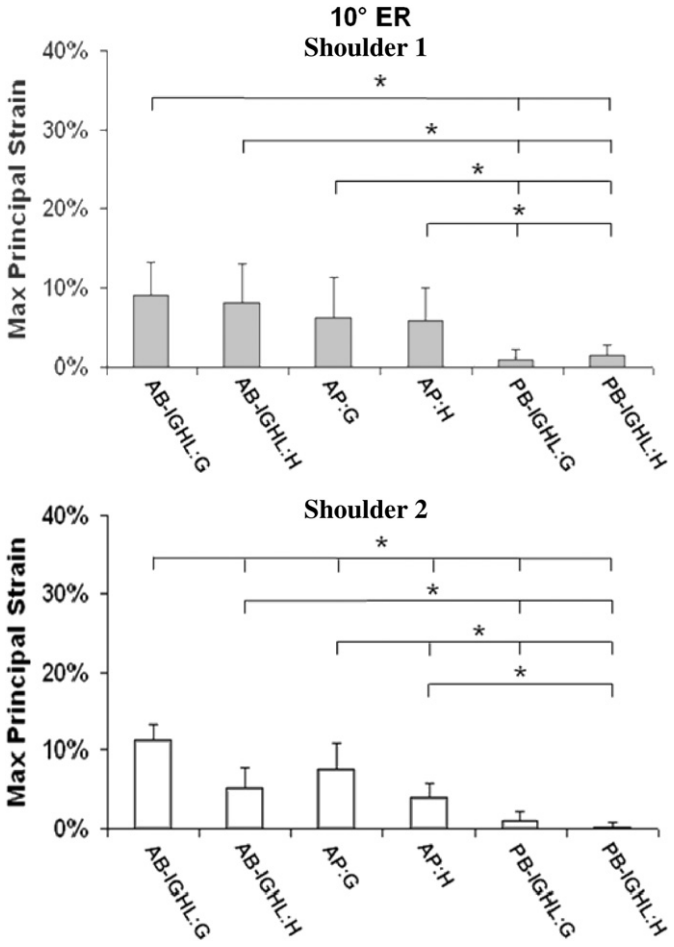

Fig. 3. Strains on the six sub-regions of Shoulder 1 and Shoulder 2, at the joint position with 10° of external rotation (* difference is statistically significant and greater than $\pm 3.5\%$ strain).

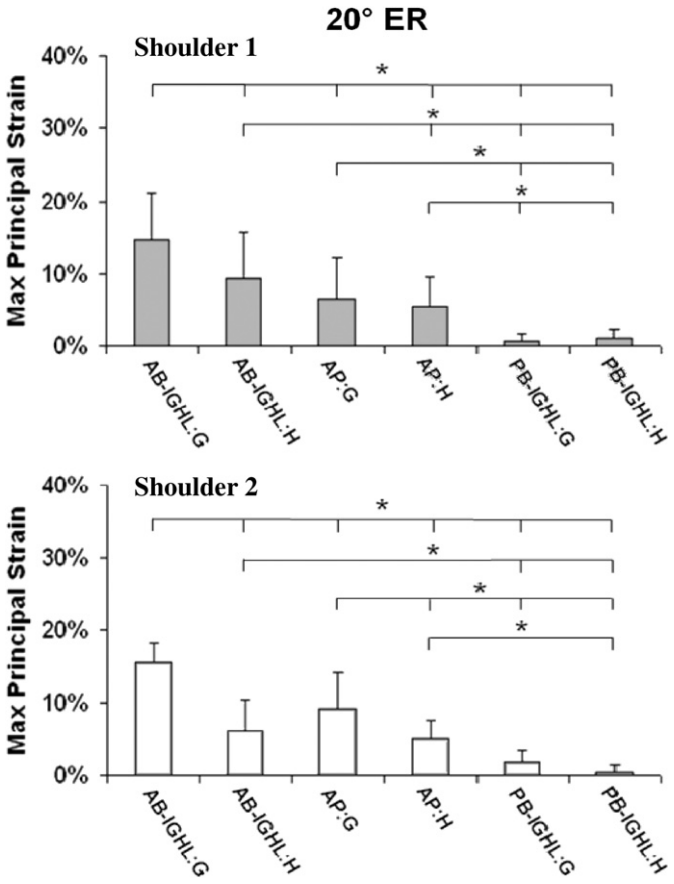

Fig. 4. Strains on the six sub-regions of Shoulder 1 and Shoulder 2, at the joint position with 20° of external rotation (* difference is statistically significant and greater than $\pm 3.5\%$ strain).

validation was performed in only the AB-IGHL, the predicted strains in the remaining sub-regions of both Shoulder 1 and Shoulder 2 were similar to the experimental strains but were not able to be used for validation due to their magnitude being less than the experimental repeatability.

The maximum sub-region strain in both Shoulder 1 (36.6% strain) and Shoulder 2 (21.7% strain) occurred on the glenoid side of the AB-IGHL at the joint position with 50° of external rotation. Therefore, the strain on each of the six sub-regions at each joint position was normalized to these values for each model, creating a strain ratio value for each sub-region at each joint position.

The correlation analysis of the strain ratios for the sub-regions of Shoulder 1 and Shoulder 2 indicated that the joint positions with 10°, 20°, 30°, and 40° of external rotation had $r^2 \geq 0.7$ ($r^2 = 0.79$, 0.87, 0.94, and 0.75, respectively), indicating a high correlation between the distribution of strain on the AIC in Shoulder 1 and in Shoulder 2 (Fig. 2). However, the joint positions with 0° and 50° of external rotation, did not have $r^2 \geq 0.7$ ($r^2 = 0.43$ and 0.59, respectively), and were thus excluded from further analyses. In addition, the joint positions with 10°, 20°, 30°, and 40° of external rotation resulted in strain on the glenoid side of the AB-IGHL in both Shoulder 1 and Shoulder 2 to be greater than 7% strain (twice the experimental repeatability), and were thus suitable for further analyses.

At the joint position with 10° of external rotation, a single sub-region of the AIC did not have significantly higher strain than the five other sub-regions in both models (Fig. 3). At the joint positions with 20°, 30°, and 40° of external rotation, however, strain on the glenoid side of the AB-IGHL was significantly higher than strain on the remaining five sub-regions in both models (Figs. 4–6, respectively). Specifically, strain on this sub-region in Shoulder 1 was greater than all other sub-regions by 5.3%, 12.5%, and 19.6% strain and in Shoulder 2 was greater than all other sub-regions by 6.3%, 6.6%, and 4.4% strain at the joint positions with 20°, 30°, and 40° of external rotation, respectively.

Strain on the glenoid side of the AB-IGHL increased with external rotation at the joint positions with 20–40° of external rotation. Furthermore, the minimum difference in strain between the glenoid side of the AB-IGHL and the remaining five sub-regions generally increased with external rotation at these joint positions (Table 2).

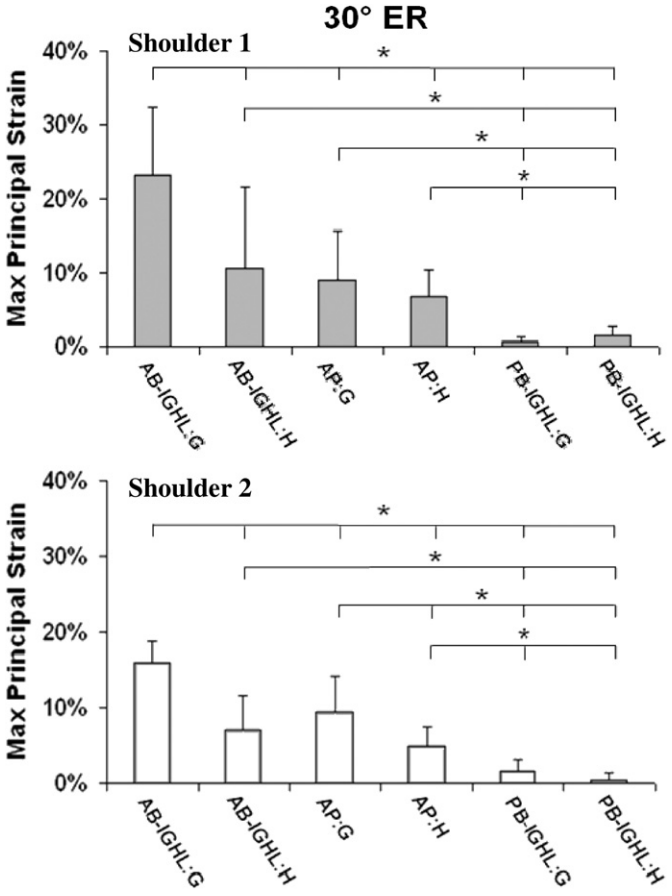

Fig. 5. Strains on the six sub-regions of Shoulder 1 and Shoulder 2, at the joint position with 30° of external rotation (* difference is statistically significant and greater than ±3.5% strain).

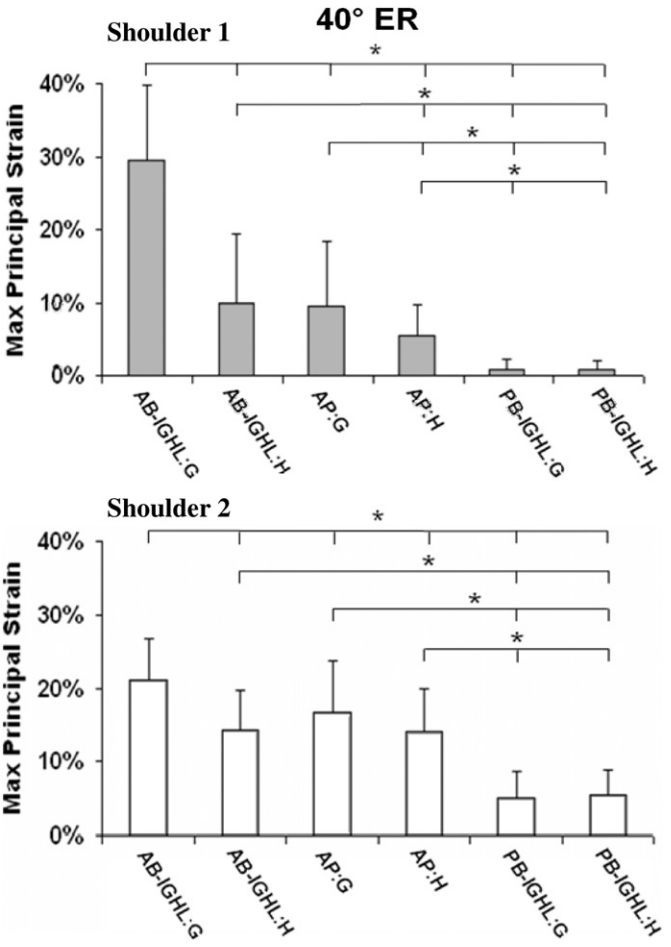

Fig. 6. Strains on the six sub-regions of Shoulder 1 and Shoulder 2, at the joint position with 40° of external rotation (* difference is statistically significant and greater than ±3.5% strain).

4. Discussion

In this study, two subject-specific finite element models of the glenohumeral joint were developed and validated by comparing experimental and predicted capsule strains at clinically relevant joint positions. The results from this study suggest that the joint positions with a 25 N anterior load applied at 60° of glenohumeral abduction and 10–40° of external rotation may result in a consistent distribution of strain and thus consistent distribution of load in the anterior-inferior capsule among subjects. Thus, standard joint positions may exist where the stability provided by the capsule is consistent among subjects. Diagnosis of capsule pathology with physical examinations has been difficult because of the large variability in glenohumeral

Table 2
Magnitude of strain (Avg ± SD) on the glenoid side of the anterior band of the inferior glenohumeral ligament as well as the minimum differences in strain when compared to the remaining five sub-regions at the joint positions with 20°, 30°, and 40° of external rotation.

External rotation (deg.)	Shoulder 1		Shoulder 2	
	Magnitude (%)	Min. differernce from sub-regions (%)	Magnitude (%)	Min. differernce from sub-regions (%)
20	14.5 ± 6.5	5.3	15.5 ± 2.7	6.4
30	23.1 ± 9.2	12.5	15.9 ± 2.7	6.6
40	29.4 ± 10.3	19.6	21.2 ± 5.7	4.4

joint size, range of motion, and allowable humeral head translations among patients. Our findings of specific joint positions at which capsule function is consistent among two subject-specific finite element models suggests that joint positions may exist within the population where effective diagnoses of capsule pathology can be made, regardless of subject variability.

The current work suggests that the glenoid side of the AB-IGHL has the greatest contribution to stability at the joint positions with a 25 N anterior load applied at 60° of glenohumeral abduction and 20–40° of external rotation. In addition, the data indicate that the relative contribution to joint stability provided by this sub-region increases with external rotation relative to the remaining five sub-regions of the anterior-inferior capsule. This data is consistent with previous work and clinical outcomes indicating that the glenoid side of the AIC may have a greater contribution to stability compared to the other capsule regions in joint positions with abduction and external rotation (Bankart, 1938; Bankart, 1923; Drury et al., 2007; Malicky et al., 2001; Moore et al., 2008) and additional studies suggesting that capsule function may be region-specific (Bigliani et al., 1992; Itoi et al., 1993; Ticker et al., 1996). Furthermore, this data is consistent with previous work performed with cadavers (Moore et al., 2008) and subject-specific finite element models (Drury et al., 2007) suggesting that strain becomes highest in the glenoid side of the AB-IGHL when the joint is abducted and externally rotated. Overall, the strains obtained at each joint position in the current work compare favorably with experimental strains obtained in five cadavers in previous work performed in our research center and in external work (Malicky et al., 2001; Moore et al., 2008). Specifically, the strain values at joint positions with 0°, 30°, and maximum external rotation are within the range of strain values obtained at corresponding joint positions in the previous study.

Despite the advancement in validation, Shoulder 1 was unable to be validated at the joint position with 0° of external rotation. The conclusions drawn using the two subject-specific finite element models may therefore be limited at joint positions with minimal amounts of external rotation. This does not affect the analyses of the current work, however, as the joint positions that were found to have important clinical significance were those with greater than 10° of external rotation. It is possible that the use of the isotropic hyperelastic constitutive model may have hindered validation at low range-of-motion joint positions, as it may underestimate strains on the capsule tissue when the capsule is loaded into its toe region (Drury, 2008). However, this constitutive model was used to successfully validate Shoulder 2 at the joint position with 0° of external rotation, and development and validation of additional models will allow further evaluation of the constitutive model's ability to represent the capsule in all joint positions. It is also worth noting that use of an isotropic hyperelastic constitutive model in the current work marks an improvement over previous work in our research center using an isotropic hypoelastic constitutive model that was only able to validate a subject-specific finite element model at a single joint position (Moore et al., 2010).

The conclusions drawn from this study are based upon the distribution of strain in two subject-specific finite element models. The distribution of strain on the capsule is complex; however, the use of six sub-regions of the AIC provided small enough areas so that average strain in each sub-region was indicative of the stability provided by that sub-region. In order to account for the variable stability provided by the capsule that exists between subjects, additional subject-specific finite element models should be developed, validated, and analyzed in the future using the current procedures. The current work, however, provides valuable insight into the effects that joint positions with abduction and increasing external rotation have on the stability provided by the capsule, and establishes the methods for development, validation, and analysis of future models.

In summary, our results suggest that anterior stability provided by the anterior-inferior capsule is consistent among subjects at joint positions with abduction and a mid-range of external rotation. The often-injured glenoid side of the anterior band of the inferior glenohumeral ligament had the greatest contribution to stability at these joint positions. Therefore, it may be possible to establish standard joint positions for physical examinations that clinicians can use to effectively diagnose pathology in the anterior-inferior capsule, which may then lead to improved outcomes after shoulder dislocation.

Conflict of interest statement

None declared.

Acknowledgement

This research was supported by NIH Grant AR-050218.

Appendix A. Supplementary materials

Supplementary data associated with this article can be found in the online version at doi:10.1016/j.jbiomech.2010.11.018.

References

Bankart, A.S., 1938. The pathology and treatment of recurrent dislocation of the shoulder joint. Br. J. Surg. 26, 23–29.
Bankart, A.S., 1923. Recurrent or habitual dislocation of the shoulder-joint. Br. Med. J. 2, 1132–1133.
Bigliani, L.U., Pollock, R.G., Soslowsky, L.J., Flatow, E.L., Pawluk, R.J., Mow, V.C., 1992. Tensile properties of the inferior glenohumeral ligament. J. Orthop. Res. 2 (10), 187–197.
Boselli, K.J., Cody, E.A., Bigliani, L.U., 2010. Open capsular shift: there is a role!. Orthop. Clin. North Am. 41 (3), 427–438.
Brenneke, S.L., Reid, J., Ching, R.P., Wheeler, D.L., 2000. Glenohumeral kinematics and capsulo-ligamentous strain resulting from laxity exams. Clin. Biomech. (Bristol, Avon) 10 (15), 735–742.

Burkart, A.C., Debski, R.E., 2002. Anatomy and function of the glenohumeral ligaments in anterior shoulder instability. Clin. Orthop. 400, 32–39.
Cadet, E.R., 2010. Evaluation of glenohumeral instability. Orthop. Clin. North Am. 41 (3), 287–295.
Cave, E., Burke, J., Boyd, R., 1974. Trauma Management. Year Book Medical Publishers, Chicago, IL 437 pp.
Cooper, D.E., Arnoczky, S.P., O'Brien, S.J., Warren, R.F., DiCarlo, E., Allen, A.A., 1992. Anatomy, histology, and vascularity of the glenoid labrum. An anatomical study. J. Bone Jt. Surg. Am. 1 (74), 46–52.
Debski, R.E., Moore, S.M., Mercer, J.L., Sacks, M.S., McMahon, P.J., 2003. The collagen fibers of the anteroinferior capsulolabrum have multiaxial orientation to resist shoulder dislocation. J. Shoulder Elbow Surg. 3 (12), 247–252.
Debski, R.E., Weiss, J.A., Newman, W.J., Moore, S.M., McMahon, P.J., 2005. Stress and strain in the anterior band of the inferior glenohumeral ligament during a simulated clinical examination. J. Shoulder Elbow Surg. 14 (1 Suppl. S), 24S–31S.
Debski, R.E., Wong, E.K., Woo, SL-Y, Sakane, M., Fu, F.H., Warner, J.J., 1999. In situ force distribution in the glenohumeral joint capsule during anterior–posterior loading. J. Orthop. Res. 5 (17), 769–776.
Drury, N., 2008. Evaluating the Anterior Stability Provided by the Glenohumeral Capsule: A Finite Element Approach. University of Pittsburgh, Pittsburgh.
Drury, N.J., Ellis, B.J., McMahon, P.J., Weiss, J.A., Debski, R.E., 2008a. The impact of glenoid labrum thickness and modulus on labrum and glenohumeral capsule pathology. In: Proceedings of the 2008 Annual Meeting of Orthopaedic Research Society, San Francisco, CA.
Drury, N.J., et al., 2008b. The inferior stability provided by the glenohumeral capsule increases with external rotation in the abducted glenohumeral joint. In: Proceedings of the ASME 2008 Summer Bioengineering Conference, SBC2008-192857, Marco Island, FL.
Drury, N.J., et al., 2007. Maximum principal strains in the glenohumeral capsule during a clinical exam: a validated finite element model. In: Proceedings of the ASME 2007 Summer Bioengineering Conference, SBC2007-175358, Keystone, CO.
Ellis, B.J., Debski, R.E., Moore, S.M., McMahon, P.J., Weiss, J.A., 2007. Methodology and sensitivity studies for finite element modeling of the inferior glenohumeral ligament complex. J. Biomech. 3 (40), 603–612.
Ellis, B.J., Drury, N.J., Moore, S.M., McMahon, P.J., Weiss, J.A., Debski, R.E., 2010. Finite element modelling of the glenohumeral capsule can help assess the tested region during a clinical exam. Comput. Meth. Biomech. Biomed. Eng. 3 (13), 413–418.
Ellis, B.J., Lujan, T.J., Dalton, M.S., Weiss, J.A., 2006. Medial collateral ligament insertion site and contact forces in the ACL-deficient knee. J. Orthop. Res. 4 (24), 800–810.
Engelmann, B.E., Whirley, R.G., Goudreau, G.L., A simple shell element formulation for large-scale elastoplastic analysis. In: Analytical and Computational Models of Shells, vol. CED-3, The American Society of Mechanical Engineers, New York, 1989.
Gerber, C., Ganz, R., 1984. Clinical assessment of instability of the shoulder with special reference to anterior and posterior drawer tests. J. Bone Jt. Surg. Br. 4 (66), 551–556.
Harryman II, D.T., Sidles, J.A., Harris, S.L., Matsen III, F.A., 1992. Laxity of the normal glenohumeral joint: a quantitative in vivo assessment. J. Shoulder Elbow Surg. 1, 66–76.
Hawkins, R.H., Hawkins, R.J., 1985. Failed anterior reconstruction for shoulder instability. J Bone Jt. Surg. Br. 5 (67), 709–714.
Hawkins, R.J., Mohtadi, N.G., 1991. Controversy in anterior shoulder instability. Clin. Orthop. Relat. Res. 272, 152–161.
Itoi, E., Grabowski, J.J., Morrey, B.F., An, K.N., 1993. Capsular properties of the shoulder. Tohoku J. Exp. Med. 3 (171), 203–210.
Kawada, T., Abe, T., Yamamoto, K., Hirokawa, S., Soejima, T., Tanaka, N., Inoue, A., 1999. Analysis of strain distribution in the medial collateral ligament using a photoelastic coating method. Med. Eng. Phys. 5 (21), 279–291.
Lusardi, D.A., Wirth, M.A., Wurtz, D., Rockwood, Jr., C.A., 1993. Loss of external rotation following anterior capsulorrhaphy of the shoulder. J. Bone Jt. Surg. Am. 8 (75), 1185–1192.
Maker, B.N., 1995. Rigid bodies for metal forming analysis with NIKE3D. Technical Report #UCRL-JC-119862, University of California, Lawrence Livermore Laboratory.
Malicky, D.M., Soslowsky, L.J., Kuhn, J.E., Bey, M.J., Mouro, C.M., Raz, J.A., Liu, C.A., 2001. Total strain fields of the antero-inferior shoulder capsule under subluxation: a stereoradiogrammetric study. J. Biomech. Eng. 5 (123), 425–431.
Matsen III, F.A., Harryman II, D.T., Sidles, J.A., 1991. Mechanics of glenohumeral instability. Clin. Sports Med. 4 (10), 783–788.
May, S., Chance-Larsen, K., Littlewood, C., Lomas, D., Saad, M., 2010. Reliability of physical examination tests used in the assessment of patients with shoulder problems: a systematic review. Physiotherapy 96 (3), 179–190.
McMahon, P.J., Dettling, J., Sandusky, M.D., Tibone, J.E., Lee, T.Q., 1999. The anterior band of the inferior glenohumeral ligament. Assessment of its permanent deformation and the anatomy of its glenoid attachment. J. Bone Jt. Surg. Br. 3 (81), 406–413.
Moore, S.M., Ellis, B., Weiss, J.A., McMahon, P.J., Debski, R.E., 2010. The glenohumeral capsule should be evaluated as a sheet of fibrous tissue: a validated finite element model. Ann. Biomed. Eng. 38 (1), 66–76.
Moore, S.M., McMahon, P.J., Azemi, E., Debski, R.E., 2005. Bi-directional mechanical properties of the posterior region of the glenohumeral capsule. J. Biomech. 6 (38), 1365–1369.
Moore, S.M., Musahl, V., McMahon, P.J., Debski, R.E., 2004. Multidirectional kinematics of the glenohumeral joint during simulated simple translation tests: impact on clinical diagnoses. J. Orthop. Res. 4 (22), 889–894.
Moore, S.M., Stehle, J.H., Rainis, E.J., McMahon, P.J., Debski, R.E., 2008. The current anatomical description of the inferior glenohumeral ligament does not correlate with its functional role in positions of external rotation. J. Orthop. Res. 26 (12), 1598–1604.
Moseley, H., Overgaard, B., 1962. The anterior capsular mechanism in recurrent anterior dislocation of the shoulder: morphological and clinical studies with special reference to the glenoid labrum and glenohumeral ligaments. J. Bone Jt. Surg. Br. 44, 913–927.
Munro, B.H., 2005. Statistical Methods for Health Care Research. Lippincott–Raven Publishers, Philadelphia, PA.
Musahl, V., Moore, S.M., McMahon, P.J., Debski, R.E., 2006. Orientation feedback during simulated simple translation tests has little clinical significance on the magnitude and precision of glenohumeral joint translations. Knee Surg. Sports Traumatol. Arthrosc. 11 (14), 1194–1199.
Newman, W.J., Debski, R.E., Gardiner, J.C., Moore, S.M., Weiss, J.A., 2002. Function of the anterior band of the inferior glenohumeral ligament during the load and shift test. In: Proceedings of the ASME Advances in Bioengineering, vol. BED-53.
O'Brien, S.J., Neves, M.C., Arnoczky, S.P., Rozbruck, S.R., Dicarlo, E.F., Warren, R.F., Schwartz, R., Wickiewicz, T.L., 1990. The anatomy and histology of the inferior glenohumeral ligament complex of the shoulder. Am. J. Sports Med. 5 (18), 449–456.
Ovesen, J., Nielsen, S., 1985. Stability of the shoulder joint. Cadaver study of stabilizing structures. Acta Orthop. Scand. 2 (56), 149–151.
Pollock, R.G., Bigliani, L.U., 1993. Recurrent posterior shoulder instability: diagnosis and treatment. Clin. Orthop. Relat. Res. 291, 85–96.
Rainis, E.J., Maas, S.A., Henninger, H.B., McMahon, P.J., Weiss, J.A., Debski, R.E., 2009. Material properties of the axillary pouch of the glenohumeral capsule: is isotropic material symmetry appropriate? J. Biomech. Eng. 3 (131), 031007.
Rockwood, C.A., Matsen III, F.A., Wirth, M.A., Harryman II, D.T., 1998. The Shoulder. W.B. Saunders Co., Philadelphia, PA.
Simo, J.C., 1988. On the dynamics in space of rods undergoing large motions: a geometrically exact approach. Comput. Meth. Appl. Mech. Eng. 66, 125–161.
Spalazzi, J.P., Gallina, J., Fung-Kee-Fung, S.D., Konofagou, E.E., Lu, H.H., 2006. Elastographic imaging of strain distribution in the anterior cruciate ligament and at the ligament-bone insertions. J. Orthop. Res. 10 (24), 2001–2010.
Ticker, J.B., Bigliani, L.U., Soslowsky, L.J., Pawluk, R.J., Flatow, E.L., Mow, V.C., 1996. Inferior glenohumeral ligament: geometric and strain-rate dependent properties. J. Shoulder Elbow Surg. 4 (5), 269–279.
Turkel, S.J., Panio, M.W., Marshall, J.L., Girgis, F.G., 1981. Stabilizing mechanisms preventing anterior dislocation of the glenohumeral joint. J. Bone Jt. Surg. Am. 8 (63), 1208–1217.
Tzannes, A., Paxinos, A., Callanan, M., Murrell, G.A., 2004. An assessment of the interexaminer reliability of tests for shoulder instability. J. Shoulder Elbow Surg. 1 (13), 18–23.